Joint multinary inversion of gravity and magnetic data using Gramian constraints

Wei Lin[1,3], and Michael S. Zhdanov[1,2]*
[1]University of Utah; [2]TechnoImaging; [3]Minmetals Exploration & Development

Summary

This paper introduces a novel approach to the joint inversion of gravity and magnetic data based on multinary transformation of the model parameters and Gramian constraints. By combining these two concepts, the joint multinary inversion using Gramian constraints not only makes it possible to explicitly exploit the sharp contrasts of the density and magnetic susceptibility between the host media and anomalous targets in the inversion of gravity and magnetic data, but also provides consistent spatial boundaries of the anomalous targets in the distributions of density and magnetic susceptibility. We demonstrate that, this method can be effectively used for the joint inversion of the full tensor gravity gradiometry (FTG) and the total magnetic intensity (TMI) data by applying the developed algorithm to the field data collected in the area of the McFualds Lake in northwestern Ontario, Canada. The joint inversion results provide a geological model with high resolution for the exploration of magmatic chromite deposits.

Introduction

Over the years, different techniques have been developed for joint inversion algorithms. For example, if the direct functional relationships between the different physical properties are known a priori, then one can apply a method based on the direct joint parameter inversion (e.g., Vozoff and Jupp, 1975). In a case where different physical properties can be expressed by different functionals of the same intrinsic pertrophysical properties (e.g. porosity, water saturation), one can invert the different observed geophysical data jointly for these intrinsic properties (e.g., Gao et al., 2012; Abubakar et al., 2012). The cross-gradient constraint is a popular solution for the joint inverse problem when the different physical properties are not correlated but have similar geometrical structures (Haber and Oldenburg, 1997; Gallardo and Meju, 2003, 2007, 2011; Colombo and De Stefano, 2007).

Zhdanov et al. (2012) introduced a unified approach to the joint inversion of different geophysical data using Gramian constraints. By imposing an additional requirement of minimizing the Gramian during the regularized inversion, one can recover multiple model parameters with enhanced correlation between the different physical properties and/or their attributes (Lin and Zhdanov, 2017).

Another complication of geophysical inversion is that, the traditional inversions of potential field data usually characterize the distributions of physical properties by a function, which varies continuously within the given bounds (Zhdanov, 2002, 2015). In order to improve the resolution of the inversions of potential field data, several techniques have been developed which aid the recovery of anomalous targets with high contrasts between physical properties and sharp boundaries (e.g., Portniaguine and Zhdanov, 1999; Zhdanov, 2002, 2015) In the papers by Zhdanov and Cox (2013) and Zhdanov and Lin (2017), the multinary inversion algorithm was proposed to explicitly exploit the sharp contrasts of the density between the host media and anomalous targets in the inversion of gravity data. This method is a generalization of binary density inversion for models described by any number of discrete model parameters (e.g. Bosch et al., 2001; Krahenbuhl and Li, 2006), or of a level set method (e.g., Osher and Sethian, 1988; Santosa, 1996; Dorn and Lesselier, 2006; Li et al., 2016).

In this paper, we propose a novel approach to the joint inversion of gravity and magnetic data based on multinary transformation of the model parameters and Gramian constraints. We have applied this method for the joint inversion of gravity and magnetic data in the area of McFaulds Lake of northwestern Ontario of Canada.

Joint inversion using Gramian constraints

Consider two different geophysical data sets, $\mathbf{d}^{(i)}$ (i=1,2), representing gravity and magnetic data, respectively, and the related two physical properties, $\mathbf{m}^{(i)}$ (i=1,2), representing density ($\boldsymbol{\rho}$) and magnetic susceptibility ($\boldsymbol{\chi}$), respectively. The joint inversion for these two model parameters can be formulated as a minimization of a single parametric functional according to the following formula (Zhdanov et al., 2012; Zhdanov, 2015):

$$P^{\alpha}\left(\mathbf{m}^{(1)},\mathbf{m}^{(2)}\right)=\sum_{i=1}^{2}\varphi^{(i)}(\mathbf{m}^{(i)})+\sum_{i=1}^{2}\alpha^{(i)}S_{MN}(\mathbf{m}^{(i)})+\beta S_G(L\mathbf{m}^{(1)},L\mathbf{m}^{(2)}). \quad (1)$$

where the coefficients $\alpha^{(i)}$ and β are some positive numbers introduced for weighting the different parts of the parametric functional; $\varphi^{(i)}$ are the misfit functionals for the weighted data:

$$\varphi^{(i)}=\left\|\mathbf{W}_d^{(i)}\left(\mathbf{A}^{(i)}\left(\mathbf{m}^{(i)}\right)-\mathbf{d}^{(i)}\right)\right\|^2, i=1,2, \quad (2)$$

and the minimum norm stabilizing functionals, S_{MN}, are calculated as follows:

$$S_{MN}^{(i)}=\left\|\mathbf{W}_m^{(i)}(\mathbf{m}^{(i)}-\mathbf{m}_{apr}^{(i)})\right\|^2, i=1,2. \quad (3)$$

In formulae (2) and (3), $\mathbf{W}_d^{(i)}$ and $\mathbf{W}_m^{(i)}$ are the data weighting and the model weighting; The term S_G is the Gramian constraint (Zhdanov et al., 2012), which in a case

10.1190/segam2018-2995792.1

of two physical properties can be written, using matrix notations, as follows:

$$S_G = \begin{vmatrix} (L\mathbf{m}^{(1)}, L\mathbf{m}^{(1)}) & (L\mathbf{m}^{(1)}, L\mathbf{m}^{(2)}) \\ (L\mathbf{m}^{(2)}, L\mathbf{m}^{(1)}) & (L\mathbf{m}^{(2)}, L\mathbf{m}^{(2)}) \end{vmatrix}, \quad (4)$$

where operator L represent some log transformation of the model parameters; and operation $(\cdot,\cdot)$ stands for the inner product of two vectors in the corresponding Gramian space (Zhdanov, 2015). By minimizing the parametric functional (1), we enforce the linear correlation between the model parameters or their transforms.

Multinary model transform

Consider a gravity inverse problem with multinary model transform. It can be formulated as a solution of the following operator equation:

$$\mathbf{d}^g = \mathbf{A}^g(\boldsymbol{\rho}), \quad (5)$$

where $\mathbf{A}^g$ is a linear operator for computing the gravity field; $\mathbf{d}^g$ are the observed gravity field data, which may include the gravity field, G_z, and all components of the full gravity gradient tensor, and $\boldsymbol{\rho}$ represents the model density. In the case of a discrete inverse problem, the density distribution $\boldsymbol{\rho}$ can be represented as a vector formed by N_m components:

$$\boldsymbol{\rho} = [\rho_1, \rho_2, \dots, \rho_{N_m}]^T, \quad (6)$$

and the observed data $\mathbf{d}$ can be considered as an N_d-dimensional vector,

$$\boldsymbol{d} = [d_1, d_2, \dots, d_{N_d}]^T, \quad (7)$$

where N_m is the number of unknown model parameters (e.g., the number of discretization cells in the inverse model); N_d is the number of data points; and superscript "T" denotes the transposition operation.

The nonlinear transformation of the continuous function into the multinary function can be described as follows. The original vector of anomalous density distribution, $\boldsymbol{\rho}$, is transformed into a new vector model space, $\tilde{\boldsymbol{\rho}} = [\tilde{\rho}_1, \tilde{\rho}_2, \dots, \tilde{\rho}_{N_m}]^T$, defined by a number of discrete densities, $\rho^{(j)}$ (j=1,2,…,P), using a superposition of error functions (i=1,2,…, N_m):

$$\tilde{\rho}_i = E_\sigma(\rho_i) = c\rho_i + \frac{1}{2}\sum_{j=1}^{P}[1 + \mathrm{erf}(\frac{\rho_i - \rho^{(j)}}{\sqrt{2}\sigma})]. \quad (8)$$

In the last formula, the error function, erf(z), is defined as follows:

$$\mathrm{erf}(z) = \frac{2}{\sqrt{\pi}}\int_0^z e^{-t^2}dt, \quad (9)$$

where parameter σ is a standard deviation of the value $\rho^{(j)}$, constant c is a small number to avoid singularities in the calculation of the derivatives of the quasi-multinary densities, $\tilde{\rho}_i$, and P is a total number of discrete values of the model parameters, $\rho^{(j)}$. The discrete densities, $\rho^{(j)}$, can be chosen a priori based on the known geological information (e.g., core samples).

Joint multinary inversion using Gramian constraints

The forward modeling of gravity and magnetic responses can be expressed by linear operators with respect to density ($\boldsymbol{\rho}$) and magnetic susceptibility ($\boldsymbol{\chi}$), as follows:

$$\mathbf{d}^g = \mathbf{A}^g(\boldsymbol{\rho}), \mathbf{d}^m = \mathbf{A}^m(\boldsymbol{\chi}), \quad (10)$$

where $\mathbf{A}^m$ is the linear forward modeling operators for magnetic fields, respectively; and $\mathbf{d}^m$ is the observed total magnetic intensity (TMI) data. For the joint inverse problem, we can rewrite equation (10) as follows:

$$\mathbf{d} = \mathbf{A}(\mathbf{m}). \quad (11)$$

In the last formula, the following notations are used: $\mathbf{d}$ is a vector of the observed gravity and magnetic data,

$$\mathbf{d} = [\mathbf{d}^g, \mathbf{d}^m]^T; \quad (12)$$

$\mathbf{m}$ is a vector of the model parameters (density and magnetic susceptibility),

$$\mathbf{m} = [\boldsymbol{\rho}, \boldsymbol{\chi}]^T; \quad (13)$$

and $\mathbf{A}$ is a combined matrix of the linear forward operators,

$$\mathbf{A} = \begin{bmatrix} \mathbf{A}^g & \\ & \mathbf{A}^m \end{bmatrix}. \quad (14)$$

As a result of the multinary model transform, the original density and magnetic susceptibility distributions, $\mathbf{m} = [\boldsymbol{\rho}, \boldsymbol{\chi}]^T$, have become the transformed distribution, $\tilde{\mathbf{m}} = [\tilde{\boldsymbol{\rho}}, \tilde{\boldsymbol{\chi}}]^T$. Therefore, the original inverse problem (11) takes the following form:

$$\mathbf{d} = \mathbf{A}[E_\sigma^{-1}(\tilde{\mathbf{m}})] = \tilde{\mathbf{A}}_\sigma(\tilde{\mathbf{m}}), \quad (15)$$

where $\tilde{\mathbf{A}}_\sigma$ is the new forward modeling operator acting in the transformed model spaces, $\tilde{\mathbf{m}}$.

By combining the multinary transformation and the Gramian constraints, we solve the inverse problem (11) based on the minimization of the following Tikhonov parametric functional:

$$P_\sigma^\alpha(\tilde{\mathbf{m}}^{(1)}, \tilde{\mathbf{m}}^{(2)}) = \sum_{j=1}^{2}\left\|\mathbf{W}_{d^{(j)}}(\tilde{\mathbf{A}}_{\sigma^{(j)}}(\tilde{\mathbf{m}}^{(j)}) - \mathbf{d}^{(j)})\right\|^2 + \sum_{j=1}^{2}\alpha^{(j)}\left\|\mathbf{W}_{m^{(j)}}(\tilde{\mathbf{m}}^{(j)} - \tilde{\mathbf{m}}_{apr}^{(j)})\right\|^2 + \beta S_G(L\tilde{\mathbf{m}}^{(1)}, L\tilde{\mathbf{m}}^{(2)}) \rightarrow \min. \quad (16)$$

We can apply the regularized conjugate gradient (RCG) method to find the global minimum of the parametric function, P_σ^α (Zhdanov, 2002, 2015).

In the case of joint multinary inversion with structural constraint, one can apply the gradient operator, $L = \nabla$, to enhance the similarities of physical boundaries of anomalous bodies.

Case study: joint inversion of gravity and magnetic data in the area of McFaulds Lake of Ontario of Canada

McFaulds Lake is located in northwestern Ontario approximately 50 km east of Webequie, where the Eagle's Nest nickel, copper and platinum group element (Ni-Cu-PGE) deposit was discovered. This area is part of a mantle-derived, highly magnetic ultramafic intrusion known as the

10.1190/segam2018-2995792.1

"Ring of Fire" that has been emplaced along the margin of a major granodiorite pluton within rocks of the Sachigo greenstone belt (Balch et al., 2010). Several economic mineral deposits have been explored in this area, including: magmatic Ni-Cu-PGE, magmatic chromite mineralization, volcanic massive sulfide mineralization and diamonds hosted by kimberlite. The Ring of Fire is composed of mafic metavolcanic flows, felsic metavolcanic flows and pyroclastic rocks and a suite of layered mafic to ultramafic intrusions that trend subparallel with and obliquely cut the westernmost part of the belt, close to a large granitoid batholith lying west of the belt. The major layered intrusion at its base, hosts Ni-Cu-PGE deposits of exceptional grade as well as overlying stratiform chromite deposits further east and higher in the layered intrusion stratigraphy (Ontario Geological Survey and Geological Survey of Canada, 2011; Zhu and Zhdanov, 2013).

Chromite deposits usually occur in layered ultramafic intrusive rocks, which is commonly associated with magnetite and serpentine. Thus, one can trace chromite magnetically through its possible host rock. On the other hand, since the density of chromitite ranges from 3.6 to 4.0 g/cm^3, chromite can be also found in the areas which have large positive gravity anomalies. Accordingly, the airborne geophysical surveys were conducted in the area of McFaulds Lake in 2010, where the airborne gravity gradiometer (AGG) and total magnetic intensity (TMI) data were collected (Ontario Geological Survey and Geological Survey of Canada, 2011). For the preliminary study, we selected a subset of the AGG and magnetic data covering the known chromite mineral, as shown in Figure 5 (adopted from Balch et al., 2010; Zhu and Zhdanov, 2013). In the target area, there are four chromite deposits: Big Daddy, Black Creek, Black Thor, and Black Label. In the following section, we will apply the gravity inversion and magnetic inversion jointly with and without multinary transformation. We will show the cross sections of two selected lines, L1 and L2 in Figure 1, which vertically cross the Black Creek.

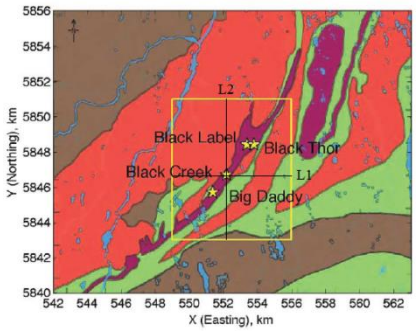

Figure 1. Target area (yellow box) of the Ring of Fire zone overlapped with regional geological sketch map (adapted from Balch et al., 2010; Zhu and Zhdanov, 2013).

Case (1): joint inversion without multinary transformation.

The size of the inversion domain was set to be 9 km × 10 km × 2 km, and the domain was discretized by prismatic cells of 50 m × 50 m × 50 m. The gravity and gravity gradiometry components, G_z, G_{xx}, G_{yy}, and G_{zz}, as well as the total magnetic intensity (TMI) component were selected for the inversions. The numbers of receivers for the gravity and magnetic surveys in the domain are 963 and 1197, respectively. The stopping criterion of normalized misfit is set as 2%. First we ran the gravity and magnetic inversions separately using the minimum norm stabilizer. The left and right columns of Figure 2 show vertical cross sections of the predicted density and magnetic susceptibility distributions along the lines, L1 and L2, respectively. The cross sections can only provide limited resolution of the geological targets.

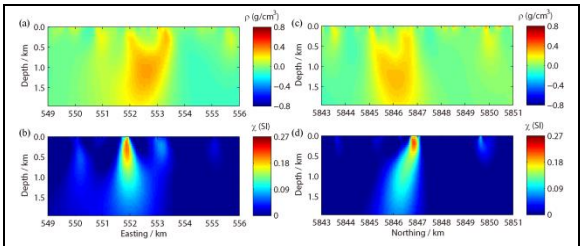

Figure 2. Case (1): Panels (a)-(b) and (c)-(d) show the vertical cross sections of the recovered anomalous density and magnetic susceptibility distributions corresponding to the lines, L1 and L2, respectively. The results were obtained from the separate inversions..

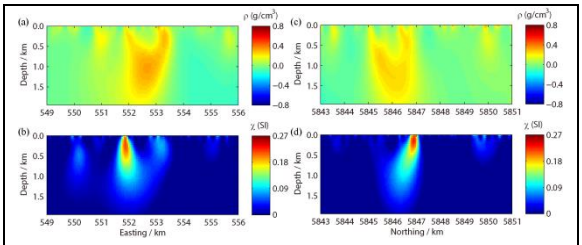

Figure 3. Case (1): Panels (a)-(b) and (c)-(d) show the vertical cross sections of the recovered anomalous density and magnetic susceptibility distributions corresponding to the lines, L1 and L2, respectively. The results were obtained from the joint inversion without multinary transformation.

We applied the joint inversion of gravity and magnetic data without multinary transformation, assuming a linear relationship between the gradients of the anomalous density and magnetic susceptibility ($L = \nabla$). Figure 3, panels (a)-(b) and (c)-(d), show the vertical cross sections of the recovered anomalous density and magnetic susceptibility distributions corresponding to lines, L1 and L2 in Figure 1, respectively. Compared to the previous results, the predicted anomalous targets become slightly compact, but overall the targets are still diffused. According to the known geological information, apparently, the centered

10.1190/segam2018-2995792.1

recovered magnetic susceptibility anomalies are associated with the Black Creek chromite deposit. However, the recovered density distribution provides a bigger anomalous body. For the mineral exploration, one may expect a more compact predicted mineral body with sharp boundary. In order to provide a convincing geological model, we applied the joint inversion with multinary transformation.

Case (2): joint inversion with multinary transformation.

In this section, we apply the joint inversion algorithm with multinary transformation and structural Gramian constraint ($L = \nabla$). Based on the known geological information (e.g., borehole data), the multinary functions were set to recover two discrete densities of 0 g/cm^3 and 0.45 g/cm^3, and two discrete magnetic susceptibilities of 0 SI and 0.2 SI (where value 0 represents the background model) with fixed standard deviations of $\sigma^{(1)} = 0.15$ and $\sigma^{(2)} = 0.06$, respectively. The representations of the multinary model transforms for anomalous density ($\boldsymbol{\rho}$) and magnetic susceptibility ($\boldsymbol{\chi}$) and their derivatives are shown in Figure 4, panels (a)-(d), respectively. The stopping criterion of the normalized misfit is also set as 2%.

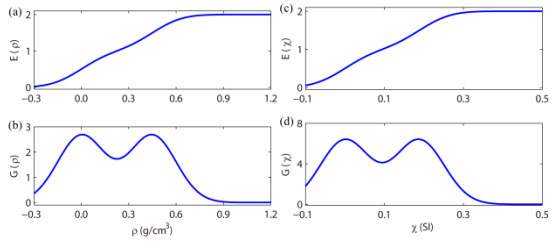

Figure 4. Case (2): Panels (a)-(b) shows the representations of the multinary model transforms for anomalous density ($\boldsymbol{\rho}$) and its derivative, respectively. Panels (c)-(d) show the corresponding plots for the magnetic susceptibility ($\boldsymbol{\chi}$).

Figure 5, panels (a)-(b) and (c)-(d) shows the vertical cross sections of the recovered anomalous density and magnetic susceptibility distributions corresponding to lines, L1 and L2 in Figure 1, respectively. For the L1 cross section, the upper boundaries of the recovered mineral body can be clearly seen from the joint inversion results, while the lower part of the body is less magnetic but much denser. For the L2 cross section, the gravity inversion result shows two vertically intrusive dykes with higher anomalous densities, while the magnetic inversion tells us that the dyke on the right contains more magnetic minerals, which corresponds to the chromite mineral in the area of Black Creek. Both cross sections provide higher resolution than the inversion results in the previous case. Compared to the previous joint inversion result, it is obvious that the novel developed joint inversion algorithm with multinary transformation provides more reasonable and direct geological features of the mineral targets.

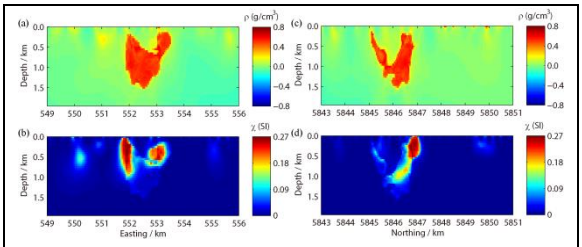

Figure 5. Case (2): Panels (a)-(b) and (c)-(d) show the vertical cross sections of the recovered anomalous density and magnetic susceptibility distributions corresponding to the lines, L1 and L2, respectively. The results were obtained from the joint inversion with multinary transformation.

Conclusion

We have developed a method of joint inversion of multimodal geophysics data based on the multinary transform and Gramian constraints. This method was applied to the problem of the joint inversion of potential fields. We have demonstrated that this inverse problem can be solved using a gradient-type optimization method. We have tested this method with 3D synthetic models, which demonstrated that the joint multinary inversion can recover the approximate sizes, locations, and the physical properties of the anomalous bodies well (considering a limited size of the abstract, these results are not shown here). We have also applied this method in the joint inversion of gravity and magnetic data collected over the McFaulds Lake area in northwestern Ontario, Canada, and the joint inversion results provided a reasonable geological model for the exploration of magmatic chromite deposits.

Acknowledgements

The authors acknowledge supports from the University of Utah's Consortium for Electromagnetic Modeling and Inversion (CEMI) and TechnoImaging. We also thank the Ontario Geological Survey and Geological Survey of Canada for providing the airborne survey data.

10.1190/segam2018-2995792.1

REFERENCES

Abubakar, A., G. Gao, T. M. Havashy, and J. Liu, 2012, Joint inversion approaches for geophysical electromagnetic and elastic full-waveform data: Inverse Problems, **28**, 055016.

Balch, S. J., J. E. Mungall, and J. Niemi, 2010, Present and future geophysical methods for Ni-Cu-PGE exploration: Lessons from McFaulds Lake, northern Ontario: Society of Economic Geologists Special Publication, **15**, 559–572.

Bosch, M., A. Guillen, and P. Ledru, 2001, Lithologic tomography: an application to geophysical data from the Cadomian belt of northern Brittany, France: Tectonophysics, **331**, 197–227, https://doi.org/10.1016/s0040-1951(00)00243-2.

Colombo, D., and M. D. Stefano, 2007, Geophysical modeling via simultaneous joint inversion of seismic, gravity, and electromagnetic data: Application to prestack depth imaging: The Leading Edge, **26**, 326–331, https://doi.org/10.1190/1.2715057.

Dorn, O., and D. Lesselier, 2006, Level set methods for inverse scattering: Inverse Problems, **22**, R67–R131, https://doi.org/10.1088/0266-5611/22/4/r01.

Gallardo, L. A., and M. A. Meju, 2003, Characterization of heterogeneous near-surface materials by joint 2D inversion of DC resistivity and seismic data: Geophysical Research Letters, **30**, 1658, https://doi.org/10.1029/2003gl017370.

Gallardo, L. A., and M. A. Meju, 2004, Joint two-dimensional DC resistivity and seismic travel time inversion with cross-gradients constraints: Journal of Geophysical Research: Solid Earth, **109**, B03311, https://doi.org/10.1029/2003jb002716.

Gallardo, L. A., and M. A. Meju, 2011, Structure-coupled multiphysics imaging in geophysical sciences: Reviews of Geophysics, **49**, RG1003, https://doi.org/10.1029/2010rg000330.

Gao, G., A. Abubakar, and T. M. Habashy, 2012, Joint petrophysical inversion of electromagnetic and full-waveform seismic data: Geophysics, **77**, no. 3, WA3–WA18, https://doi.org/10.1190/geo2011-0157.1.

Haber, E., and D. Oldenburg, 1997, Joint inversion: a structural approach: Inverse Problems, **13**, 63–77, https://doi.org/10.1088/0266-5611/13/1/006.

Krahenbuhl, R. A., and Y. Li, 2006, Inversion of gravity data using a binary formulation: Geophysical Journal International, **167**, 543–556, https://doi.org/10.1111/j.1365-246x.2006.03179.x.

Lin, W., and M. S. Zhdanov, 2017, Joint inversion of seismic and gravity gradiometry data using Gramian constraints: Annual International Meeting, SEG, Expanded Abstracts, 1734–1738, https://doi.org/10.1190/segam2017-17650942.1.

McMillan, M. S., C. Schwarzbach, E. Haber, and D. Oldenburg, 2015, 3D parametric hybrid inversion of time-domain airborne electromagnetic data: Geophysics, **80**, no. 6, K25–K36, https://doi.org/10.1190/geo2015-0141.1.

Ontario Geological Survey and Geological Survey of Canada, 2011, Ontario airborne geophysical surveys, gravity gradiometer and magnetic data, grid and profile data (ASCII and Geosoft(R) formats) and vector data, McFaulds Lake area: Ontario Geological Survey, Geophysical Data Set 1068.

Osher, S., and J. A. Sethian, 1988, Fronts propagating with curvature-dependent speed: algorithms based on Hamilton-Jacobi formulations: Journal of Computational Physics, **79**, 12–49, https://doi.org/10.1016/0021-9991(88)90002-2.

Portniaguine, O., and M. S. Zhdanov, 1999, Focusing geophysical inversion images: Geophysics, **64**, 874–887, https://doi.org/10.1190/1.1444596.

Santosa, F., 1996, A level set approach for inverse problems involving obstacles: ESAIM: Control, Optimisation and Calculus of Variations, **1**, 17–33, https://doi.org/10.1051/cocv:1996101.

Vozoff, K., and D. L. B. Jupp, 1975, Joint inversion of geophysical data: Geophysical Journal of the Royal Astronomical Society, **42**, 977–991, https://doi.org/10.1111/j.1365-246x.1975.tb06462.x.

Zhdanov, M. S., 2002, Geophysical inverse theory and regularization problems: Elsevier.

Zhdanov, M. S., 2009, New advances in regularized inversion of gravity and electromagnetic data: Geophysical Prospecting, **57**, 463–478, https://doi.org/10.1111/j.1365-2478.2008.00763.x.

Zhdanov, M. S., A. Gribenko, and G. Wilson, 2012, Generalized joint inversion of multimodal geophysical data using Gramian constraints: Geophysical Research Letters, **39**, L09301, https://doi.org/10.1029/2012gl051233.

Zhdanov, M. S., and L. Cox, 2013, Multinary inversion of geophysical data: Proceedings of the Annual Meeting of the Consortium for Electromagnetic Modeling and Inversion, The University of Utah, 125–136.

Zhdanov, M. S., 2015, Inverse theory and applications in geophysics: Elsevier.

Zhdanov, M. S., and W. Lin, 2017, Adaptive multinary inversion of gravity and gravity gradiometry data: Geophysics, **82**, no. 6, G101–G114, https://doi.org/10.1190/geo2016-0451.1.

Zheglova, P., and C. Farquharson, 2018, Multiple level-set joint inversion of traveltime and gravity data with application to ore delineation: A synthetic study: Geophysics, **83**, no. 1, R13–R30, https://doi.org/10.1190/geo2016-0675.1.

Zhu, Y., and M. S. Zhdanov, 2013, Gramian constraints in the joint inversion of airborne gravity gradiometry and magnetic data: Proceedings of the Annual Meeting of the Consortium for Electromagnetic Modeling and Inversion, The University of Utah, 97–124, https://doi.org/10.1190/segam2013-0735.1.

Zhu, Y., 2017, Joint inversion of potential field and electromagnetic data using Gramian constraints: Doctoral dissertation, The University of Utah.